

Proglacial river sediment fluxes in the south-eastern Tibetan Plateau: Ming Yong Glacier in the Upper Mekong River

XiXi Lu¹, Ting Zhang², Boey Lai Hsia³, Dongfeng Li¹, Heather Fair⁴, Samuel Chua¹, Li Li³, and Shaojuan Li³

¹National University Singapore Department of Geography

²Affiliation not available

³Yunnan University of Finance and Economics

⁴University of Minnesota Twin Cities

March 28, 2022

Abstract

Glacial and proglacial erosion are important sediment sources in a river basin. The retreat of many glaciers on the Tibetan Plateau has important implications on the supply of fresh water and sediment dynamics for downstream river basins. Despite the importance of water and sediment dynamics at these catchments, existing quantification of suspended sediment fluxes from glacial catchments on the Tibetan Plateau is limited due to poor accessibility and challenging environments. This study presents the results of in-situ investigations of water discharge and suspended sediment fluxes from the Ming Yong glacial catchment in Yunnan, Southwest China, between August 2013 and July 2017. The results show that the variation in water discharge and suspended sediment was highly seasonal. The variation of average suspended sediment concentration was large – 69 ± 45 mg/L; 119 ± 104 mg/L; 94 ± 97 mg/L in 2013, 2015, 2016, respectively. We estimate that the sediment yield from Ming Yong catchment was highly variable ranging from 1104 t/km²/year in 2013 to 2281 t/km²/year in 2016, with 65-78% of the total annual sediment load occurring during summer (June to August). These annual variations in the sediment yield can be attributed largely to precipitation patterns, or otherwise, extreme melting events. This study has provided a benchmark dataset that can be used for further works that investigate the impact of climate change on sediment dynamics in glacierized catchments in the Tibetan Plateau. Subsequently, the study let us better understand the increasing sediment supply to the Upper Mekong River from glacierized catchments.

Proglacial river sediment fluxes in the south-eastern Tibetan Plateau: Ming Yong Glacier in the Upper Mekong River

¹Xixi Lu, ¹Ting Zhang, ²Boey Lai Hsia, ¹Dongfeng Li, ^{3,4,5}Heather Fair, ¹Samuel DX Chua, ²Li Li, ²Shaojuan Li

¹Department of Geography, National University of Singapore, 10 Kent Ridge Crescent, Singapore 119260, Singapore

²School of Urban Management and Resource Environment, Yunnan University of Finance and Economics, 237 Long Quan Road, Kunming 650221, China

³National Science Foundation Postdoctoral Research Fellow in Biology, University of Minnesota

⁴Institute of Mountain Hazards and Environment, Chinese Academy of Sciences, Chengdu, China

⁵USDA Agricultural Research Service, 590 Woody Hayes Drive, Columbus, OH, 43210, USA.

Corresponding to Xixi Lu (geoluxx@nus.edu.sg); Ting Zhang (zhang.ting@u.nus.edu)

Abstract

Glacial and proglacial erosion are important sediment sources in a river basin. The retreat of many glaciers on the Tibetan Plateau has important implications on the supply of fresh water and sediment dynamics for downstream river basins. Despite the importance of water and sediment dynamics at these catchments, existing quantification of suspended sediment fluxes from glacial catchments on the Tibetan Plateau is limited due to poor accessibility and challenging environments. This study presents the results of in-situ investigations of water discharge and suspended sediment fluxes from the Ming Yong glacial catchment in Yunnan, Southwest China, between August 2013 and July 2017. The results show that the variation in water discharge and suspended sediment was highly seasonal. The variation of average suspended sediment concentration was large – 69 ± 45 mg/L; 119 ± 104 mg/L; 94 ± 97 mg/L in 2013, 2015, 2016, respectively. We estimate that the sediment yield from Ming Yong catchment was highly variable ranging from 1104 t/km²/year in 2013 to 2281 t/km²/year in 2016, with 65-78% of the total annual sediment load occurring during summer (June to August). These annual variations in the sediment yield can be attributed largely to precipitation patterns, or otherwise, extreme melting events. This study has provided a benchmark dataset that can be used for further works that investigate the impact of climate change on sediment dynamics in glacierized catchments in the Tibetan Plateau. Subsequently, the study let us better understand the increasing sediment supply to the Upper Mekong River from glacierized catchments.

Introduction

The meltwater from glaciers on the Tibetan Plateau feeds many large Asian rivers, for example, Indus, Ganges, Brahmaputra, Salween, Mekong, Tarim, Syr Darya (Li et al., 2021). Millions of people in the region depend on the rivers for their livelihoods. With an average elevation exceeding 3,000m, the Tibetan Plateau contains around 36,800 glaciers occupying a total area of ~50,000 km² (Yao et al., 2012). These physical conditions caused the Tibetan Plateau to be more susceptible to solar insolation and amplified its sensitivity to global warming (Pepin et al., 2015). Indeed, Yao et al. (2012) found that glacial retreat on the Tibetan Plateau has intensified since the 1990s.

Glaciers are powerful agents of erosion through denudation mechanisms, generating large amounts of glacial debris in the process. Thus, sediment yields from glacial basins are higher than the global average (Hallet et al., 1996). Suspended sediment fluxes from proglacial areas, accompanied by intensified meltwater and increased sediment availability, have increased in response to accelerated glacier retreat (Li et al., 2021; Overeem et al., 2017). In glacier regions, the roles of sediment are double-edged – while it is essential in the maintenance of riverine ecology, morphology, agriculture, and fisheries by providing nutrients and materials (Walling, 2006), sediments absorb toxic chemicals such as mercury. Therefore, high concentrations of sediment degrade water quality, change aquatic habitats, and cause civil engineering problems for dams and river transportation (Li et al., 2021). Furthermore, given the context of climate change, understanding sediment dynamics from glacial catchments, such as the Tibetan Plateau, is important for land resource management and planning (Li et al., 2021).

Sediment transport vary spatially along a proglacial river and is characterized by strong seasonal and diurnal variabilities (Beylich et al., 2017). Proglacial sediment is predominantly produced by glacial movements and transported by glacial meltwater, from the melting of ice on the ice surface (supraglacial), at the bed (subglacial), or within the glacier (englacial) (Heckmann et al., 2016). Heat required to melt the ice can be supplied by solar radiation or geothermal heat beneath the glacier (Bennett & Glasser, 2011). Therefore, proglacial discharge hydrographs follow the temporal changes in solar incidence on annual and diurnal timescales (Miles et al., 2020). Also, the rates at which meltwater and sediment are drained depend on the type of pathways and the channel size (Carrivick & Tweed, 2021).

Previous studies on the quantification of suspended sediment load on the Tibetan Plateau are mostly derived from hydrological gauging stations that are located far away from the glaciers (Li et al., 2021; Shi et al., 2018). Also, field measurements of suspended sediment fluxes from proglacial rivers in the Tibetan Plateau are very limited and spatially scattered. For example, Kumar et al. (2002) measured discharge and suspended

sediment in the meltwater of Gangotri Glacier in Garhwal Himalaya, India; Kireet et al. (2012) analyzed the spatio-temporal trends of suspended sediment flux along the Sutlej River and its main tributaries in western Himalaya; Srivastava et al. (2014) measured discharge and suspended sediment load at Dunagiri Glacier basin located in Garhwal Himalaya between 1984 and 1989. Nearer to Southeast Asia, studies that examined sediment loads in the Mekong basin have reported a lack of sediment data from the Upper Mekong located within China (Lu and Siew, 2006; Walling, 2008; Wang et al., 2011). Particularly, the glaciated catchments there are poorly studied and, to our best knowledge, there has not been any study done to quantify the sediment load there.

Consequently, this study focuses on Ming Yong Glacier in Yunnan Province, which is located in the southeast region on the Tibetan Plateau. The glacier was found to have retreated by 190m between 1998 and 2004, with 110m of the retreat occurring between 2002 and 2004 (Baker & Moseley, 2007). Against this reduction, knowledge about sediment delivery from the glacial catchments in the Upper Mekong basin is ever more important in the understanding of sediment delivery dynamics for the whole Mekong basin (Lu et al., 2014). Therefore, this study aims to: (1) quantify the sediment yield and sediment load from the Ming Yong glacial catchment; (2) analyze the temporal variability of suspended sediment flux from Ming Yong glacial catchment; and (3) discuss the potential drivers and implications of changing sediment yield for the Upper Mekong basin in the context of climate change.

2. Study Area

Ming Yong Glacier is a valley glacier situated in Deqin County, Yunnan Province in Southwest China (Figure 1). Flowing from the east face of the Meili Snow Mountain Range, this glacial catchment was selected due to its location on the south-eastern edge of the Tibetan Plateau that renders it particularly sensitive to climate change. Being part of the Three Parallel Rivers of Yunnan – the upper reaches of Yangtze, Mekong, and Salween – this area has received much attention from environmental conservationists due to its rich biodiversity and diverse ecosystems. Ming Yong Glacier flows from the east face of the Meili Snow Mountain Range into the Upper Mekong River (also known as the Lancang River). Thereafter, the Mekong continues its journey into the riparian countries of Myanmar, Laos, Thailand, Cambodia, and Vietnam. The total length of the Mekong is 4,350 km with a total drainage area of 795,000 km².

The study area has a catchment area of 39.7 km² with 27 km² covered by glaciers (68%). The elevation of the watershed ranges from 6684m at the Kawargarbo Peak to 2930m at the glacier terminus with an average slope of 29% (Figure S1). The Ming Yong glacial icefall is covered by a layer of supraglacial moraine and debris that is contributed by sediments from the steep valley sides (Figure 2b). From the glacial terminus to the confluence with the Upper Mekong River, the Ming Yong River flows for about 6.1 km. Due to accessibility issues, water samples and discharge measurements were taken from a single sampling station 3.1 km from the glacial terminus at an elevation of 2342 m (Figure S1). Specifically, the sampling station is located at 28°28'5.80"N, 98°46'58.57"E.

Ming Yong catchment is classified as a monsoon-influenced temperate oceanic climate – dry winter and a warm, wet summer – under the Köppen-Geiger climate classification (Beck et al., 2018). At least 70% of its average annual precipitation is received during the warmest months (Figure 2c-d). Due to the lack of a weather station at Ming Yong, annual climate data was taken from the nearest weather station 13km away at Deqin. The average annual temperature is 5.6°C and the average annual precipitation of 641mm. Precipitation ranges from 6mm in December to 133mm in July. The average temperature is lowest at -2.2°C in January and 12.7°C in July. Variation in annual temperature is approximately 14.9°C with its coldest month in January (-2.2°C) and warmest month in July 12.7°C.

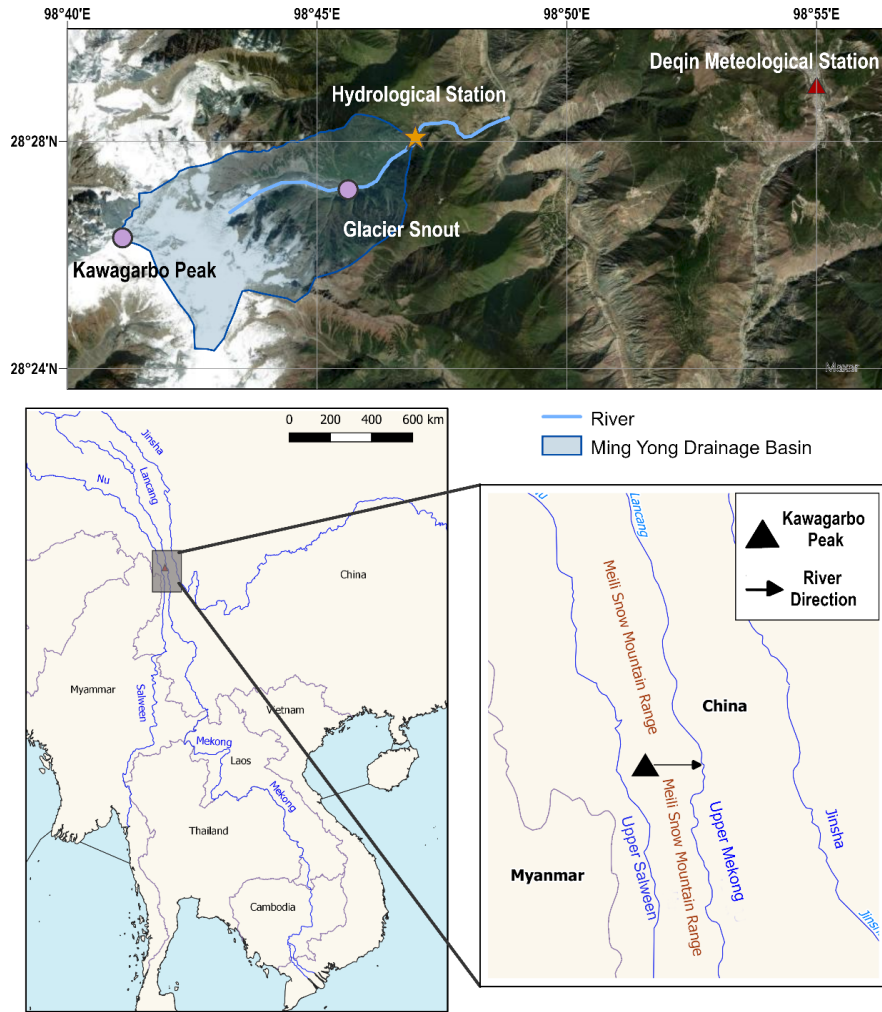


Figure 1 Location map of study area. Ming Yong glacial catchment from Google Earth (top), the Three-Parallel-River region (the upper Yangtze, the Upper Mekong and the Upper Salween) (bottom left), and the Meili Snow Mountain between the Upper Mekong River (Lancang River) and the Upper Salween River (Nu River)

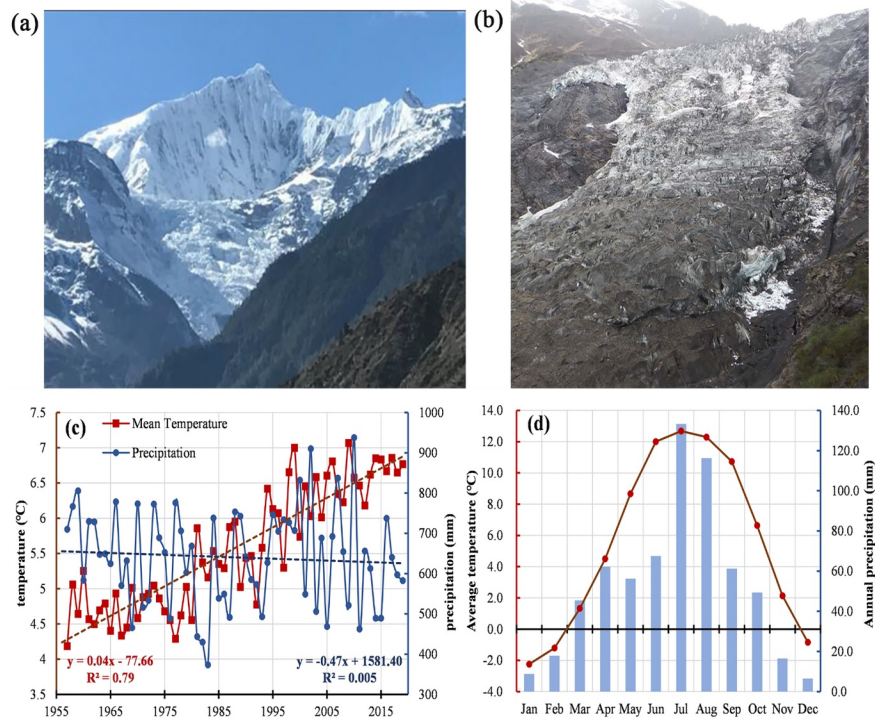


Figure 2 Geomorphic and climatic characteristics. (a) field photo of Kawagarbo Peak. (b) field photo of Ming Yong glacier icefall covered with layer of supraglacial moraine and debris. (c) Long term changes in temperature and precipitation and (d) Monthly variations in temperature and precipitation near the study site at Deqing.

3. Data and methods

3.1 Measurement of discharge

Ming Yong River itself does not have a stream gauging station, hence the discharge was manually measured and calculated (Figure S2). Flow velocity and water depth were measured during each sampling event using the float method (Figure S2a) and meter rule (Figure S2b) respectively. The cross-sectional area of the channel was measured in February 2014, September 2015, November 2016, and April 2017 (Figure S2c) because of danger when conducting measurements during the high-flow summer. To calculate the cross-sectional area, the width of the river channel under bankful conditions was first measured using a tape measure. The width was divided into 20 transacts and the height of the tape measure to the riverbed was measured at each transact. The cross-sectional area was thus obtained by the sum of all transacts (height*width of transact). Discharge was then calculated using the following formula:

$$Q = A \cdot V$$

where Q is water discharge (in m^3/s), A is the cross-sectional area of the river channel (in m^2), and V is the flow velocity (in m/s).

3.2 Water samples collection

Because a significant proportion of suspended sediment is transported during infrequent high flows (Mao et al., 2019), the frequency of collection was higher during periods of high flow to capture the high transport rates. Following the average monthly precipitation and temperature (Figure 2d), at least 5 samples were collected during periods of high flows from April to September while at least 2 samples were collected during

periods of low flows from October to March. In total there were 158 sampling events from August 2013 to July 2017 with a gap from September 2014 to August 2015 due to manpower and logistical constraints.

3.3 Measurement of suspended sediment concentration (SSC)

Except near the riverbed, mixing of suspended sediments streams is fairly homogenous throughout the cross-section. Thus, collection of water samples was done at a turbulent section to allow vertical and horizontal mixing of sediments. The sampling bottles were fully submerged and capped when fully filled. Three 500 ml water samples were collected per sampling event. Each bottle of water sample was filtered using 0.45 μm pore size, 47 mm-diameter Whatman nylon membrane filters, and a Nalgene vacuum pump and filtration unit. The filter papers were air-dried for three days in the field to remove moisture before being individually stored in aluminium foil and resealable plastic bags. Then, suspended sediment mass was obtained in the laboratory by weighing the dried samples. The average mass of suspended sediment per sampling event (mg/500ml) was multiplied by 2 to obtain the average SSC in mg/L.

3.4 Sediment rating curves

Strong correlation is often observed between suspended sediment concentration and discharge in most streams. Compared to large river systems that usually contain an abundance of materials, the suspended load of small mountain streams usually depends on episodic events that transport fine materials from banks and upland areas. Thus, suspended sediment concentration depends on both supply of sediments and discharge (Yaksich & Verhoff, 1983; Zhang et al., 2021). Nonetheless, suspended sediment concentration and discharge can be plotted to create what is known as a sediment rating curve. One benefit of developing a sediment rating curve is that it can be applied to interpolate missing data during the observation period (Asselman, 2000). Here, the sediment rating curve is a power function expressed as:

$$\text{SSC} = a \times Q^b$$

where SSC is in mg/L, Q is the water discharge (in m^3/s), and a and b are fitting coefficients.

When $b > 1$, the increase in sediment volume per 1 unit of flow volume can be nonlinear. Such situations imply that more than half of the sediment load is carried by high flows that account for less than 15% of the water volume or less than 5% of the period of measurement.

Another characteristic of suspended sediment concentration during high flow is their increased variability. Both factors indicate that more sampling should take place during periods of high discharge. However, one common limitation of suspended sediment data from small mountainous catchments is the lack of measurements conducted during high flows. Storms make access difficult and measurements hazardous. Nevertheless, high-resolution data collected during high flows are essential for the development of good sediment rating curves. Due to the infrequency of high flows and logistical problems, collecting adequate high flow measurements cannot be achieved through hand sampling alone.

Suspended sediment rating curves were determined for Ming Yong glacial catchment using discharge and suspended sediment concentration data between August 2013 and July 2017. The rating curves were fit by nonlinear least-squares curve fitting using the Levenberg-Marquardt (L-M) algorithm produced in Origin 2021b. One of the major limitations of the sediment rating curve is the assumption that the rating coefficients will remain constant (Zhang et al., 2021). As mentioned by Yaksich and Verhoff (1983), small mountainous catchment often results in “event response” streams, which causes large scatter between sediment concentration and discharge and hence poorer relationships between suspended sediment concentration and discharge. The low accuracy of the sediment rating curves may be attributed partly to hysteretic effects, where at a given discharge, the sediment concentration on the rising and falling stage of the hydrograph differs (Khan-choul & Jansson, 2008). Separate rating curves are needed for the rising and falling limbs to account for seasonal variations so as to enhance the accuracy of the estimated suspended sediment concentration (Khan-choul & Jansson, 2008). In this study, the hydrological year is defined as August to July, with the rising stage (February-July) and falling stage (August-January in the next year).

3.5 Estimation of sediment fluxes and sediment yields

Water discharge values were interpolated using a linear equation between the two closest sampling dates to obtain the daily sediment load for days without measurements. Due to interannual variation in SSC dynamics, rating curves derived using data from the falling and rising stages of the respective hydrological years were used to calculate the daily sediment load. The sediment load (SL; tons/day) was calculated using the following formula:

$$SL = Q \times SSC$$

where Q is the water discharge (in m^3/s) and SSC is the suspended sediment concentration (in mg/L). The monthly sediment load was derived by summing estimated daily sediment load for the respective month.

Sediment yield is defined as the amount of sediment per unit area removed from a watershed for a specific period of time. The sediment yield of a drainage basin, measured in tonnes/ km^2 per annum, is the resultant effects of erosion, transportation and deposition occurring in the basin, and reflects the sediment delivery ratio within. Here, the sediment yield was calculated by dividing the annual sediment load by the size of Ming Yong catchment area.

4. Results

4.1 Suspended sediment concentrations and sediment rating curves

During the study period from August 2013 to July 2017 (Figure 3), the maximum discharge was $36.1 m^3/s$ recorded on 1 August 2014, while the minimum discharge was $2.1 m^3/s$ on 10 Jan 2017. The highest SSC ($547.73 mg/L$) was recorded on 1 August 2016, and the lowest SSC ($0.2 mg/L$) was recorded on 24 January 2017. Discharge-weighted mean SSC across the entire study period was $129.4 mg/L$. Based on the hydrograph, the rising limb was between February and July and the falling limb continues from August to January in the next year. The discharge and suspended sediment data were characterized by distinct seasonal variations (Figure 3). February accounts for the lowest monthly average discharge of $3.89 m^3/s$ and January accounts for the lowest monthly average SSC of $17.7 mg/L$. Discharge begins to increase in March and reaches the peak in July, with the average discharge in July of $31.85 m^3/s$ and the highest average SSC of $261.8 mg/L$.

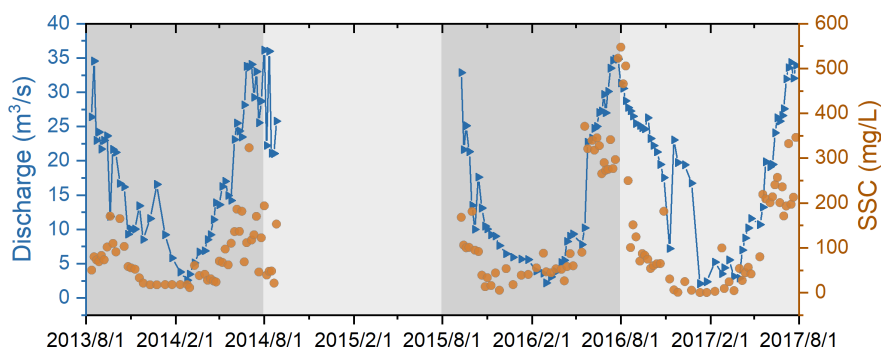


Figure 3 Observations of discharge and suspended sediment concentration (SSC) during three hydrological years. Observations of the discharge are represented by blue triangles and observations of SSC are represented by orange dots.

The R^2 value for the SSC-Q rating curve for the entire study period was relatively low at 0.40 ($p < 0.05$; Figure 4a). The SSC-Q relation exhibited a large scatter for SSC for discharge values above $25 m^3/s$. Due to the poor fit, the rating curve was fitted by hydrological years to analyze the differences between each hydrological year (Figure 4b-d). The empirical relationship between SSC and discharge improved when the data was divided by hydrological years (Figure 4b-d). In particular, the largest R^2 value can be found in the hydrological year of 2015 ($R^2=0.62$). Scatter plots for 2015 and 2016 showed distinct power-law increases in SSC for discharge above $20m^3/s$.

For discharge above $25\text{m}^3/\text{s}$ (Figure 4b-d), which were recorded during ablation seasons, large scatters were observed for all 3 hydrological years. The data was further analyzed by considering its inter-annual seasonal variations (Figure S3 and Table 1). Subsequently, the SSC-Q relationship improved when the data was categorized into falling and rising stages throughout the study period. However, during the falling stage from August 2013 to January 2014, there was still no significant correlation between discharge and SSC ($R^2= 0.11$). The coefficient of correlation was higher during the rising stage than the falling stage for all hydrological years.

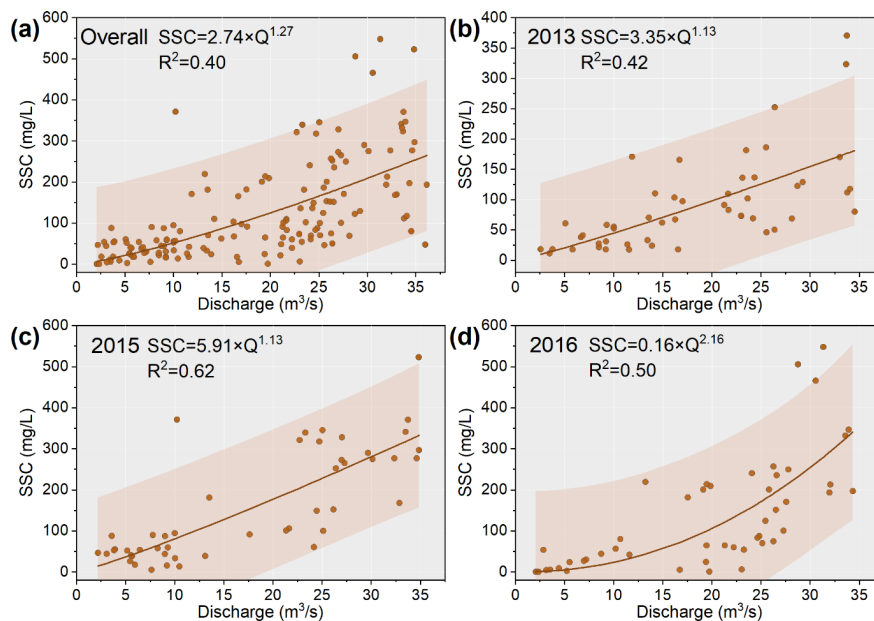


Figure 4 Suspended sediment concentration (SSC)-discharge (Q) rating curves, during (a) August 2013 to July 2017; (b) August 2013 to July 2014; (c) August 2015 to July 2016; (d) August 2016 to July 2017. The brown lines represent the sediment rating curves fitted by the corresponding SSC-Q scatter. The shaded area indicates a 95% confidence interval.

Table 1 Sediment rating curves during the falling and rising stages at Ming Yong River

Year	Sediment rating curve in the falling stage (Aug-Jan)	R^2	Sediment rating curve in the rising stage (Feb-Jul)	R^2
2013	$SSC=5.2474 \times Q^{0.8612}$	0.11	$SSC= 4.9034 \times Q^{0.9942}$	0.42
2015	$SSC=2.0104 \times Q^{1.3156}$	0.67	$SSC=15.6770 \times Q^{0.8858}$	0.62
2016	$SSC=0.0360 \times Q^{2.4087}$	0.57	$SSC=1.4774 \times Q^{1.5286}$	0.50

4.2 SSC-Q hysteresis

Temporal analyses on discharge and suspended sediment concentrations was conducted to understand the behaviour of the suspended sediment hysteresis loops. In this study, hysteresis loops were plotted based on the average monthly Q values against SSC values to obtain the variability patterns (Figure 5). Hysteresis loops for the 3 hydrological years were represented by clockwise hysteresis (Figure 5a-c), with a higher SSC-value on the rising limb than that for the same discharge on the falling limb. For instance, at the discharge of $25\text{ m}^3/\text{s}$, SSC was higher during the rising stage as compared to the falling stage (110 mg/L versus 80 mg/L in 2013, 288 mg/L versus 153 mg/L in 2015, and 220 mg/L versus 90 mg/L in 2016). The patterns across the 3 hydrological years suggest the sediment availability is depleted by the end of the ablation season (the

beginning of the falling limb), resulting in clockwise hysteresis loops. For clarity, the clockwise hysteresis loop for the entire 2016 is shown in Figure 5d.

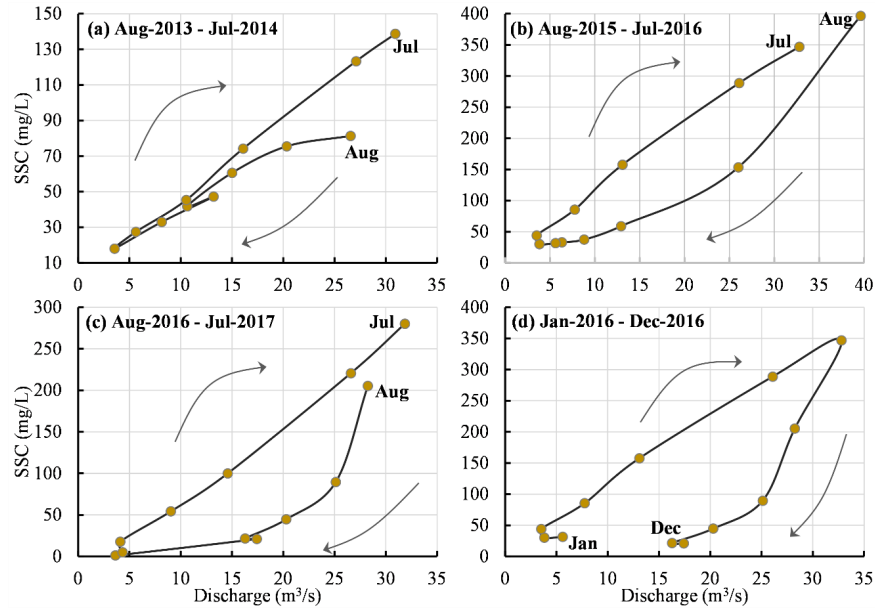


Figure 5 Suspended sediment concentration (SSC)-discharge hysteresis loops for Ming Yong catchment across three hydrological years and one calendar year. (a-c) Hysteresis in the hydrological year of 2013, 2015, and 2016, respectively; (d) Hysteresis in the calendar year of 2016. The starting month and ending month are marked for each hysteresis loop.

Hysteresis loops provide information on the influence of different sources of runoff on suspended sediment transport within proglacial rivers (Williams, 1989), by depicting the relationship between the transport capacity of the river and its sediment supply (Zhang et al., 2021). For example, sediment that is stored during periods of low discharge and transported when discharge increases results in the SSC-Q pattern in the form of a loop rather than a straight line (Smith & Dragovich, 2009). The higher SSC during the rising limb of the hydrograph compared to the falling limb may be explained by proximal sediment sources during the rising limb, but insufficient sediment supply during the falling limb (Smith & Dragovich, 2009; Williams, 1989). For Ming Yong basin, the sediment are sourced from the large amounts of debris generated by the glacial environment that are readily available for transport (Figure 2). However, during the falling stage, the suspended sediment concentrations tends to be lower due to the unavailability of sediment sources and the increase in base flow discharge from subsurface soils.

4.3 Temporal variations of water discharges and sediment yields

Both water discharge and suspended sediment flux in Ming Yong catchment are characterised by seasonal variations (Figure 6). The monthly maximum sediment loads, all occurring in July, amounted to 12.5 kt (2014), 30.3 kt (2016), and 25.1 kt (2017). Of the total annual sediment load, the majority (65% in 2013, 73% in 2015, and 78% in 2016) was highly concentrated in summer from June to August. In contrast, the dry season month of February has the lowest monthly load at around 0.25% of the total annual load.

Concurrently, the monthly sediment load was significantly correlated with the monthly water discharge, with the R^2 value of 0.82. The high sediment load during periods of high discharge suggests the predominance of supraglacial and subglacial sediment mobilization. However, more studies are still needed to differentiate the transport of sediment load by meltwater or that by precipitation.

The water discharge for hydrological years 2013, 2015, and 2016 – 0.50 km³/year, 0.46 km³/year, and 0.53 km³/year, respectively – did not vary significantly, implying little variations in annual water discharge for the Ming Yong catchment. However, annual sediment load variability was large, ranging from 44 kilotons (kt) in 2013 to 91 kt in 2015, and 73 kt in 2016 (Figure 7). Together, the sediment yield for Ming Yong glacial catchment was derived to be 1104 t/km²/year in 2013, 2281 t/km²/year in 2015, and 1833 t/km²/year in 2016.

. The high variation of annual suspended sediment yield might be induced by what is known as threshold effect in sediment transport, with disproportionally high sediment delivery efficacy in excess of the critical level (Lane & Nienow, 2019). Also, the type of substrate and subglacial deposits, rates of glacier movement, characteristics of the glacier drainage system, and the basin topography can affect the interannual variability of sediment yields (Herman et al., 2021). The competing effects of these confounding factors can be further investigated in a future study.

5. Discussion

5.1 Dominant control of sediment fluxes: temperature or precipitation?

The seasonal variations in discharge and sediment load are jointly controlled by air temperature and summer rainfall (Figure 7). At the Ming Yong Glacier, fractures in the ice form crevasses, providing pathways for surface water to penetrate the glacier (Miles et al., 2020). In summer, elevated air temperatures increase the surface melting and generate snow-glacier meltwater (Lau et al., 2010). The meltwater can flow from the surface to base through glacier conduits (Eyles, 2006), leading to higher meltwater flow velocity and capacity. As a result, there is an increase in meltwater erosion and sediment export (Delaney & Adhikari, 2020; Mao & Carrillo, 2017). Concurrently, the intense rainfall in July from the Indian monsoon increases the rate of exposed slope erosion and can trigger landslides and rock avalanches, leading to the observed high sediment loads (Table S1) (Kirschbaum et al., 2020; Rosser, 2010). In other words, the discharge and suspended sediment load peaks observed in July can be explained by higher sediment accessibility, mobilization, and transport from the monsoon rainfall. Conversely in winter, reduced snow/glacier melting and the decreased rainfall causes the deformation of the glacial conduits. Furthermore, accumulated snow shield the underlying crevasses (Carrillo & Mao, 2020; Gatesman, 2017), thereby weakening erosion and reducing the transport of sediments into the proglacial stream. (Table S1).

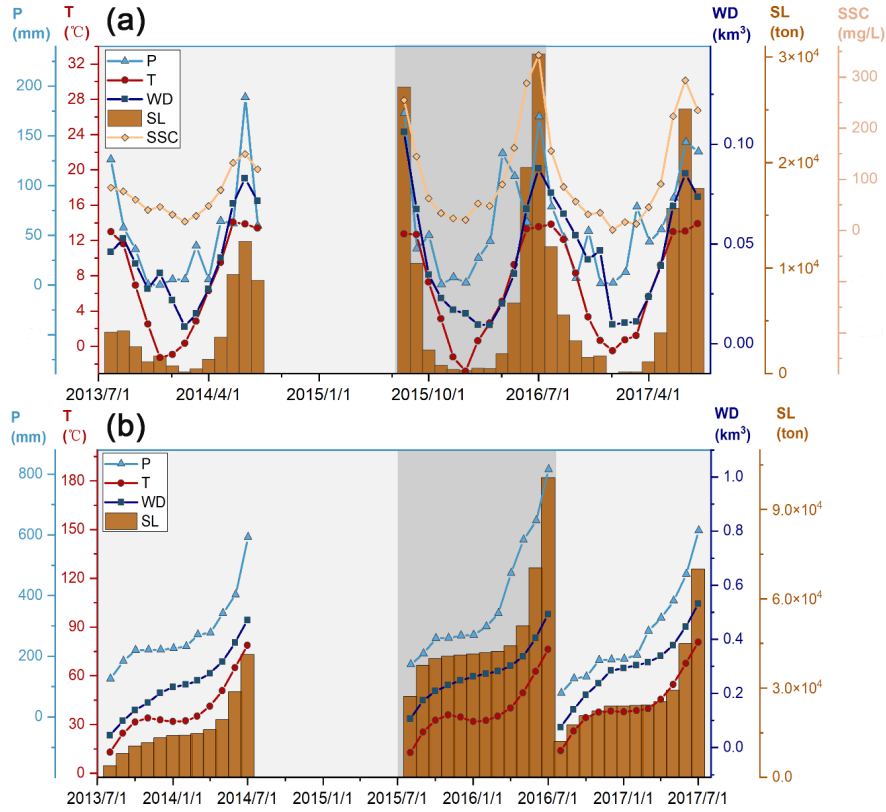


Figure 6 Monthly precipitation (P), temperature (T), water discharge (WD), sediment load (SL), and suspended sediment concentration (SSC) in Ming Yong catchment. Figure 6a shows the monthly values while Figure 6b shows the cumulative monthly values.

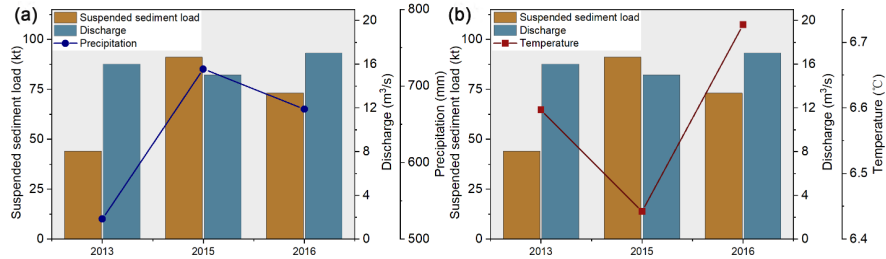


Figure 7 Annual sediment load (brown bars), water discharge (gray-blue bars), precipitation (blue line), and temperature (red line) in Ming Yong catchment across the three hydrological years.

Our observations show that there are large interannual variations of suspended sediment flux among the three hydrological years (2013, 2015, and 2016). The highest sediment yield occurred in 2015 (2283 t/km²/year)—more than doubled the sediment yield in 2013 (1104 t/km²/year). These interannual variations seem to be mainly driven by the differences in annual precipitation, rather than the mean annual temperature (Figure 6). Specifically, the highest annual precipitation was recorded in 2015, accompanied by a doubling of the number of extreme precipitation days (defined as daily precipitation over 20 mm) in Deqin meteorological station. During a wetter hydrological year, the overall increased rainfall can increase the sediment transport capacity and evacuate more deposited sediments from supra/sub-glacial debris and glacier valleys, causing a higher annual sediment yield (Delaney et al., 2018; Li 2020; Micheletti & Lane, 2016). Concurrently,

more frequent rainstorms enhance stream power and erosivity, thus increasing river channel erosion that can (re-)mobilize deposited sediments. (Li et al. 2021; Lugon & Stoffel, 2010; Wulf et al., 2010). These extreme sediment events contribute disproportionately to the annual sediment yield and amplify the temporal variability in sediment transport (Lloyd et al., 2016; Wulf et al., 2012).

Simultaneously, temperature-sensitive glacier dynamics may also affect interannual variability in sediment yield (Costa et al., 2018; Stott & Mount, 2007). For example, the rate of glacier bedrock erosion or subglacial/proglacial sediment transport can be enhanced by the increased glacier melt flow due to higher temperatures (Herman et al., 2021; Singh et al., 2020; Chakrapani & Saini, 2009; Stott & Mount, 2007). However, the temperature variations detected within our study period pales in comparison to precipitation changes. Therefore, in the absence of extreme melting events that could shadow the impact of precipitation, we argue that the interannual variations in the sediment yield in Ming Yong catchment are largely determined mostly by precipitation

5.2 Comparisons with other proglacial catchments

The sediment yield for Ming Yong glacial catchment is relatively high as compared to the those recorded from other glacierized basins on the Tibetan Plateau (Figure 8). In the Tibetan Plateau, sediment yields from glacierized basins generally decreases with increasing basin area (Figure 8a), but increases with larger glacier coverage (Figure 8b), in line with what is observed at a global scale (Milliman & Farnsworth, 2011). The high sediment yield of Ming Yong glacial catchment can be explained by its small but heavily glacierized (68%) basin area and the short distance between the sampling station and glacier snout (Hallet et al., 1996; Wulf et al., 2012). The observed inverse relationship between sediment load and basin area might be because larger basins have poorer sediment delivery ratio – due to increased sediment storage and weakened sediment connectivity (Walling, 1983; Wohl et al., 2019).

Furthermore, small glacierized basins generate disproportionately high sediment yield, because a high transport efficacy can be sustained by short sediment transport distance, steep valley gradients or high stream power of glacier melt flow (Gurnell et al., 1996; Wulf et al., 2012). In the Ming Yong glacial catchment, the sampling station is only 3 km downstream of the glacier snout and the slope ranges from 9 to 71% (Figure S1a). Apart from its physical setting, the relatively high precipitation in Ming Yong catchment (over 600 mm/year) also contributes to its high sediment mobilization and yield (Table 2). For example, the summer rainfall can flush the supraglacial debris cover and proglacial sediment storage in large volumes downstream (Riihimaki, 2005; Srivastava et al., 2014). Increased snowmelt and rainfall during the onset of the thaw season can also increase water infiltration from surface to base and enhance the subglacial drainage system, thereby facilitating the export of subglacial sediment (Alley et al., 1997; Delaney & Adhikari, 2020).

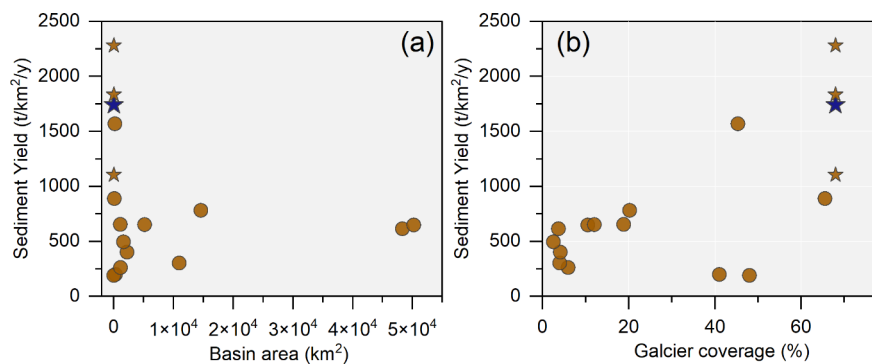


Figure 8 Sediment yields versus (a) catchment areas and (b) glacier coverage in percentage. The sediment yields of brown dots are collected from previous publications. Brown stars represent the sediment yields observed during three individual hydrological years and blue star represent the averaged sediment yield during three hydrological years in the Ming Yong catchment (in this study).

Table 2 Locations and hydroclimatic characteristics of sediment yield observations from Tibetan Plateau glacierized basins.

Basin	Observation period	Lat. (°N)	Lon. (°E)	Temperature (°C)	Precipitation (mm)
MingYong	2013	28.47	98.78	6.6	526
MingYong	2015	28.47	98.78	6.4	722
MingYong	2016	28.47	98.78	6.7	670
Keqikar River	2018	41.81	80.17	0.6	456
Rongbu River	2018	27.98	86.92	3.9	266
Kalasu River	1960-2004	42	82	7.4	125
Pishan River	1960-2016	37.22	78.77	7.0	174
Santun River	1960-2016	43.72	86.92	7.8	278
Manas River	1959-2007	44	85.77	6.0	200
Bayingou River	1983-2008	44.02	84.98	4.5	291
Yulongkashi River	1960-2010	37	79.03	-7.5	323
Yerkang River	1960-2017	37.98	76.9	-4.7	234
Shule River	1960-2016	39.82	96.25	5.0	54
Urumqi glacier No.1 catchment	2004-2008	43.1	86.82	-5.9	504
Sutlej River	2001-2009	39.82	78	-	-
Hailuogou basin	2008, 2013	29.57	101.98	4.6	1881

5.3 Implications for the Lower Mekong River

Our quantification of sediment fluxes from Ming Yong glacial catchment provides baseline measurements to better understand changes in erosion rates within the context of wider climatic alterations (Li et al., 2021). As the Ming Yong glacial region is part of the upper reach of the Mekong River and Salween River, our study also provides insights into the contribution of sediment to the upper reaches of these transboundary rivers under the fast pace of temperature increase (Figure 2c). For the Mekong Basin, better understanding of sediment supply and delivery in its entire reach is needed for better management of its sediment fluxes. One major issue is the potential impacts of Chinese dams in the Mekong River. Before Manwan Dam was constructed in 1992, the upper Mekong reach in China provided around 80 million tons of sediment to the lower reach (Lu and Siew, 2006; Wang et al., 2011; Lu et al., 2015). However, the high sediment supply from the proglacial catchments in the headwater region cannot be transported downstream because of the series of cascade dams constructed in the Upper Mekong River. According to Sun et al. (2022), the sediment load below these cascade dams in Yunnan has dropped to around 10% of the pre-dam level. Subsequently, the problem of sediment starvation due to the reservoirs trapping will get worse in future with more dams being planned or built. Further down the Mekong Basin, this declining sediment flux, in combination with regional sand-mining and water withdrawal for irrigations, has contributed to drastic water level reductions in the Cambodian floodplains and Vietnamese delta (Lu and Chua, 2021; Chua et al., 2022).

6. Conclusions

The Ming Yong glacier catchment in the upper Mekong basin is characterized by distinct wet and dry seasons, with discharge and suspended sediment concentrations (SSC) increasing from February to July and decreasing from August to January. The yearly variations in sediment load for Ming Yong glacier are large (44 kt in 2013 to 91 kt in 2015, and 73 kt in 2016), despite small variations in water discharge. More than 65% of the annual sediment load is contributed between June and August. These observed seasonal variations in the sediment load indicate the complex competing influences of the supply and storage of suspended sediment load. Specifically, the clockwise hysteresis relationship suggest that sediment is stored during the low flow season and transported when flow increased from February to July, with the exhaustion of sediment supply after July. Even though discharge and SSC are generally positively correlated, seasonal variations result in different sediment rating relationships due to the influence of glacial meltwater. Based on the in-situ

observations over three hydrological years, the sediment yields are estimated to be 1104 t/km²/year in 2013, 2283 t/km²/year in 2015, and 1833 t/km²/year in 2016.

This study provides baseline measurements for potential future monitoring of the glacial catchment in response to climate change. Concurrently, the data fills the knowledge gap in sediment data for the headwaters of the Mekong River. As this study was conducted in-situ, data was collected manually. For instance, the collection of water samples for filtration or the measurements of water depth could introduce random errors. Thus, the use of specific hydrology equipment in subsequent studies such as data loggers or turbidity meters can increase the sampling frequency and accuracies of future sediment load estimates. Furthermore, installation of a nearby weather monitoring station can give more insight into the diurnal and seasonal ablation patterns of the Ming Yong Glacier, allowing better attribution of the variation in its discharge or transport capacity to climatic or other environmental factors.

ACKNOWLEDGEMENT

The first author, Lu Xixi, would like to express his sincere thanks to Professor Des Walling for his support, encouragements and inspirations over many years. This study was supported by the National University of Singapore (R-109-000-227-115) and the Yunnan University of Finance and Economics. The work was also supported by the studentship awarded to Boey Lai Hsia from the Yunnan University of Finance and Economics. We want to thank Professor Zhou Yue, Yunnan University of Finance and Economics, for his support to our work in Yunnan. We also want to thank Professor Bruce Webb for his invitation and editing the special issue.

References

- Alley, R. B., Cuffey, K. M., Evenson, E. B., Strasser, J. C., Lawson, D. E., & Larson, G. J. (1997). How glaciers entrain and transport basal sediment: Physical constraints. *Quaternary Science Reviews*, 16 (9), 1017-1038. doi:[https://doi.org/10.1016/S0277-3791\(97\)00034-6](https://doi.org/10.1016/S0277-3791(97)00034-6)
- Asselman, N. E. M. (2000). Fitting and interpretation of sediment rating curves. *Journal of Hydrology*, 234 (3), 228-248. doi:[https://doi.org/10.1016/S0022-1694\(00\)00253-5](https://doi.org/10.1016/S0022-1694(00)00253-5)
- Baker, B. B., & Moseley, R. K. (2007). Advancing Treeline and Retreating Glaciers: Implications for Conservation in Yunnan, P.R. China. *Arctic, Antarctic, and Alpine Research*, 39 (2), 200-209. doi:10.1657/1523-0430(2007)39[200:Atargi]2.0.Co;2
- Beck, H. E., Zimmermann, N. E., McVicar, T. R., Vergopolan, N., Berg, A., & Wood, E. F. (2018). Present and future Koppen-Geiger climate classification maps at 1-km resolution. *Scientific Data*, 5 . doi:10.1038/sdata.2018.214
- Bennett, M. M., & Glasser, N. F. (2011). *Glacial geology: ice sheets and landforms* : John Wiley & Sons.
- Beylich, A. A., Laute, K., & Storms, J. E. A. (2017). Contemporary suspended sediment dynamics within two partly glacierized mountain drainage basins in western Norway (Erdalen and Bødalen, inner Nordfjord). *Geomorphology*, 287 , 126-143. doi:10.1016/j.geomorph.2015.12.013
- Carrillo, R., & Mao, L. (2020). Coupling Sediment Transport Dynamics with Sediment and Discharge Sources in a Glacial Andean Basin. *Water*, 12 (12). doi:10.3390/w12123452
- Carrivick, J. L., & Tweed, F. S. (2021). Deglaciation controls on sediment yield: Towards capturing spatio-temporal variability. *Earth-Science Reviews*, 221 . doi:10.1016/j.earscirev.2021.103809
- Chakrapani, G. J., & Saini, R. K. (2009). Temporal and spatial variations in water discharge and sediment load in the Alaknanda and Bhagirathi Rivers in Himalaya, India. *Journal of Asian Earth Sciences*, 35 (6), 545-553. doi:10.1016/j.jseaes.2009.04.002.
- Chua, S. D. X., Lu, X. X., Oeurng, C., Sok, T., & Grundy-Warr, C. (2022). Drastic decline of flood pulse in the Cambodian floodplains (Mekong River and Tonle Sap system). *Hydrology and Earth System Sciences*

, 26(3), 609-625.

Costa, A., Molnar, P., Stutenbecker, L., Bakker, M., Silva, T. A., Schlunegger, F., . . . Girardclos, S. (2018). Temperature signal in suspended sediment export from an Alpine catchment. *Hydrology and Earth System Sciences*, 22 (1), 509-528. doi:10.5194/hess-22-509-2018

Delaney, I., & Adhikari, S. (2020). Increased Subglacial Sediment Discharge in a Warming Climate: Consideration of Ice Dynamics, Glacial Erosion, and Fluvial Sediment Transport. *Geophysical Research Letters*, 47 (7). doi:10.1029/2019gl085672

Delaney, I., Bauder, A., Werder, M. A., & Farinotti, D. (2018). Regional and Annual Variability in Subglacial Sediment Transport by Water for Two Glaciers in the Swiss Alps. *Frontiers in Earth Science*, 6 . doi:10.3389/feart.2018.00175

Eyles, N. (2006). The role of meltwater in glacial processes. *Sedimentary Geology*, 190 (1-4), 257-268. doi:10.1016/j.sedgeo.2006.05.018

Gatesman, T. A. (2017). *Glacier contribution to lowland streamflow: a multi-year, geochemical hydrograph separation study in sub-Arctic Alaska* : University of Alaska Fairbanks.

Gurnell, A., Hannah, D., & Lawler, D. (1996). Suspended sediment yield from glacier basins. *IAHS Publications-Series of Proceedings and Reports-Intern Assoc Hydrological Sciences*, 236 , 97-104.

Hallet, B., Hunter, L., & Bogen, J. (1996). Rates of erosion and sediment evacuation by glaciers: A review of field data and their implications. *Global and Planetary Change*, 12 (1), 213-235. doi:https://doi.org/10.1016/0921-8181(95)00021-6

Heckmann, T., McColl, S., & Morche, D. (2016). Retreating ice: research in pro-glacial areas matters. *Earth Surface Processes and Landforms*, 41 (2), 271-276. doi:10.1002/esp.3858

Herman, F., De Doncker, F., Delaney, I., Prasicek, G., & Koppes, M. (2021). The impact of glaciers on mountain erosion. *Nature Reviews Earth & Environment*, 2 (6), 422-435. doi:10.1038/s43017-021-00165-9

Khanchoul, K., & Jansson, M. B. (2008). Sediment Rating Curves Developed on Stage and Seasonal Means in Discharge Classes for the Mellah Wadi, Algeria. *Geografiska Annaler. Series A, Physical Geography*, 90 (3), 227-236.

Kirschbaum, D., Kapnick, S. B., Stanley, T., & Pascale, S. (2020). Changes in Extreme Precipitation and Landslides Over High Mountain Asia. *Geophysical Research Letters*, 47 (4). doi:10.1029/2019gl085347

Kumar, K., Miral, M. S., Joshi, V., & Panda, Y. S. (2002). Discharge and suspended sediment in the meltwater of Gangotri Glacier, Garhwal Himalaya, India. *Hydrological Sciences Journal*, 47 (4), 611-619. doi:10.1080/02626660209492963

Lane, S. N., & Nienow, P. W. (2019). Decadal-Scale Climate Forcing of Alpine Glacial Hydrological Systems. *Water Resources Research*, 55 (3), 2478-2492. doi:10.1029/2018wr024206

Lau, W. K. M., Kim, M.-K., Kim, K.-M., & Lee, W.-S. (2010). Enhanced surface warming and accelerated snow melt in the Himalayas and Tibetan Plateau induced by absorbing aerosols. *Environmental Research Letters*, 5 (2). doi:10.1088/1748-9326/5/2/025204

Li, D., Li, Z., Zhou, Y., & Lu, X. (2020). Substantial Increases in the Water and Sediment Fluxes in the Headwater Region of the Tibetan Plateau in Response to Global Warming. *Geophysical Research Letters*, 47 (11), e2020GL087745. doi:https://doi.org/10.1029/2020GL087745

Li, D., Lu, X., Overeem, I., Walling, D. E., Syvitski, J., Kettner, A. J., . . . Zhang, T. (2021). Exceptional increases in fluvial sediment fluxes in a warmer and wetter High Mountain Asia. *Science*, 374 (6567), 599-603. doi:doi:10.1126/science.abi9649

- Li, D., Overeem, I., Kettner, A. J., Zhou, Y., & Lu, X. (2021). Air Temperature Regulates Erodible Landscape, Water, and Sediment Fluxes in the Permafrost-Dominated Catchment on the Tibetan Plateau. *Water Resources Research*, *57* (2), e2020WR028193. doi:10.1029/2020WR028193
- Li, X., Ding, Y., Liu, Q., Zhang, Y., Han, T., Jing, Z., . . . Liu, S. (2019). Intense Chemical Weathering at Glacial Meltwater-Dominated Hailuoguo Basin in the Southeastern Tibetan Plateau. *Water*, *11* (6). doi:10.3390/w11061209
- Li, Z., Gao, W., Zhang, M., & Gao, W. (2012). Variations in suspended and dissolved matter fluxes from glacial and non-glacial catchments during a melt season at Urumqi River, eastern Tianshan, central Asia. *CATENA*, *95* , 42-49. doi:10.1016/j.catena.2012.03.002
- Lloyd, C. E. M., Freer, J. E., Johnes, P. J., & Collins, A. L. (2016). Using hysteresis analysis of high-resolution water quality monitoring data, including uncertainty, to infer controls on nutrient and sediment transfer in catchments. *Sci Total Environ*, *543* (Pt A), 388-404. doi:10.1016/j.scitotenv.2015.11.028.
- Lu, X. X., & Siew, R. Y. (2006). Water discharge and sediment flux changes over the past decades in the Lower Mekong River: possible impacts of the Chinese dams. *Hydrology and Earth System Sciences* , *10*(2), 181-195.
- Lu, X.X., Kumm, M., Oeurng, C. (2014). Reappraisal of sediment dynamics in the Lower Mekong River, Cambodia. *Earth Surface Processes & Landforms* , *39*(14): 1855-1865. DOI:10.1002/esp.3573
- Lu, X. X., & Chua, S. D. X. (2021). River Discharge and Water Level Changes in the Mekong River: Droughts in an Era of Mega-Dams. *Hydrological Processes* , *35*(7), e14265.
- Lugon, R., & Stoffel, M. (2010). Rock-glacier dynamics and magnitude–frequency relations of debris flows in a high-elevation watershed: Ritigraben, Swiss Alps. *Global and Planetary Change*, *73* (3-4), 202-210. doi:10.1016/j.gloplacha.2010.06.004
- Mao, L., & Carrillo, R. (2017). Temporal dynamics of suspended sediment transport in a glacierized Andean basin. *Geomorphology*, *287* , 116-125. doi:10.1016/j.geomorph.2016.02.003
- Mao, L., Comiti, F., Carrillo, R., & Penna, D. (2019). Sediment Transport in Proglacial Rivers. In T. Heckmann & D. Morche (Eds.), *Geomorphology of Proglacial Systems: Landform and Sediment Dynamics in Recently Deglaciated Alpine Landscapes* (pp. 199-217). Cham: Springer International Publishing.
- Micheletti, N., & Lane, S. N. (2016). Water yield and sediment export in small, partially glaciated Alpine watersheds in a warming climate. *Water Resources Research*, *52* (6), 4924-4943. doi:10.1002/2016wr018774
- Miles, K. E., Hubbard, B., Irvine-Fynn, T. D. L., Miles, E. S., Quincey, D. J., & Rowan, A. V. (2020). Hydrology of debris-covered glaciers in High Mountain Asia. *Earth-Science Reviews*, *207* . doi:10.1016/j.earscirev.2020.103212
- Milliman, J. D., & Farnsworth, K. L. (2011). Runoff, erosion, and delivery to the coastal ocean. In J. D. Milliman & K. L. Farnsworth (Eds.), *River Discharge to the Coastal Ocean: A Global Synthesis*(pp. 13-69). Cambridge: Cambridge University Press.
- Overeem, I., Hudson, B. D., Syvitski, J. P. M., Mikkelsen, A. B., Hasholt, B., van den Broeke, M. R., . . . Morlighem, M. (2017). Substantial export of suspended sediment to the global oceans from glacial erosion in Greenland. *Nature Geoscience*, *10* (11), 859-863. doi:10.1038/ngeo3046
- Pepin, N., Bradley, R. S., Diaz, H. F., Baraer, M., Caceres, E. B., Forsythe, N., . . . Mountain Research Initiative, E. D. W. W. G. (2015). Elevation-dependent warming in mountain regions of the world. *Nature Climate Change*, *5* (5), 424-430. doi:10.1038/nclimate2563
- Riihimäki, C. A. (2005). Sediment evacuation and glacial erosion rates at a small alpine glacier. *Journal of Geophysical Research*, *110* (F3). doi:10.1029/2004jf000189

- Rosser, N. J. (2010). Landslides and Rockfalls. In *Sediment Cascades* (pp. 55-87).
- Shi, X., Zhang, F., Lu, X., Wang, Z., Gong, T., Wang, G., & Zhang, H. (2018). Spatiotemporal variations of suspended sediment transport in the upstream and midstream of the Yarlung Tsangpo River (the upper Brahmaputra), China. *Earth Surface Processes and Landforms*, *43* (2), 432-443. doi:10.1002/esp.4258
- Singh, A. T., Sharma, P., Sharma, C., Laluraj, C. M., Patel, L., Pratap, B., . . . Thamban, M. (2020). Water discharge and suspended sediment dynamics in the Chandra River, Western Himalaya. *Journal of Earth System Science*, *129* (1). doi:10.1007/s12040-020-01455-4
- Smith, H. G., & Dragovich, D. (2009). Interpreting sediment delivery processes using suspended sediment-discharge hysteresis patterns from nested upland catchments, south-eastern Australia. *Hydrological Processes*, *23* (17), 2415-2426. doi:10.1002/hyp.7357
- Srivastava, D., Kumar, A., Verma, A., & Swaroop, S. (2014). Characterization of suspended sediment in Meltwater from Glaciers of Garhwal Himalaya. *Hydrological Processes*, *28* (3), 969-979. doi:10.1002/hyp.9631
- Stott, T., & Mount, N. (2007). Alpine proglacial suspended sediment dynamics in warm and cool ablation seasons: Implications for global warming. *Journal of Hydrology*, *332* (3-4), 259-270. doi:10.1016/j.jhydrol.2006.07.001
- Sun, L., Sun, Z., Li, Z., Zheng, H., Li, C., & Xiong, W. (2022). Response of runoff and suspended load to climate change and reservoir construction in the Lancang River. *Journal of Water and Climate Change*.
- Wang, J. J., Lu, X. X., & Kumm, M. (2011). Sediment load estimates and variations in the Lower Mekong River. *River Research and Applications*, *27*(1), 33-46.
- Walling, D.E., 1983. The sediment delivery problem. *Journal of Hydrology*, *65*(1): 209-237. DOI:[https://doi.org/10.1016/0022-1694\(83\)90217-2](https://doi.org/10.1016/0022-1694(83)90217-2)
- Walling, D. E. (2006). Human impact on land-ocean sediment transfer by the world's rivers. *Geomorphology*, *79* (3-4), 192-216. doi:10.1016/j.geomorph.2006.06.019
- Walling, D. E. (2008). The changing sediment load of the Mekong River. *Ambio* , 150-157.
- Williams, G. P. (1989). Sediment concentration versus water discharge during single hydrologic events in rivers. *Journal of Hydrology*, *111* (1), 89-106. doi:[https://doi.org/10.1016/0022-1694\(89\)90254-0](https://doi.org/10.1016/0022-1694(89)90254-0)
- Wohl, E., Brierley, G., Cadol, D., Coulthard, T. J., Covino, T., Fryirs, K. A., . . . Sklar, L. S. (2019). Connectivity as an emergent property of geomorphic systems. *Earth Surface Processes and Landforms*, *44* (1), 4-26. doi:10.1002/esp.4434
- Wulf, H., Bookhagen, B., & Scherler, D. (2010). Seasonal precipitation gradients and their impact on fluvial sediment flux in the Northwest Himalaya. *Geomorphology*, *118* (1-2), 13-21. doi:10.1016/j.geomorph.2009.12.003
- Wulf, H., Bookhagen, B., & Scherler, D. (2012). Climatic and geologic controls on suspended sediment flux in the Sutlej River Valley, western Himalaya. *Hydrology and Earth System Sciences*, *16* (7), 2193-2217. doi:10.5194/hess-16-2193-2012
- Yaksich, S. M., & Verhoff, F. H. (1983). Sampling Strategy for River Pollutant Transport. *Journal of Environmental Engineering*, *109* (1), 219-231. doi:doi:10.1061/(ASCE)0733-9372(1983)109:1(219)
- Yao, T., Thompson, L., Yang, W., Yu, W., Gao, Y., Guo, X., . . . Joswiak, D. (2012). Different glacier status with atmospheric circulations in Tibetan Plateau and surroundings. *Nature Climate Change*, *2* (9), 663-667. doi:10.1038/nclimate1580

Zhang, T., Li, D., Kettner, A. J., Zhou, Y., & Lu, X. (2021). Constraining Dynamic Sediment-Discharge Relationships in Cold Environments: the Sediment-Availability-Transport (SAT) Model. *Water Resources Research* . doi:10.1029/2021wr030690

Zhao, Y., Ma, W., Han, H., Zhuang, S., Shi, H., Ding, Y., . . . Lu, X. (2021). Suspended Sediment Transport Characteristics of Glacial Rivers in Alpine Mountainous Areas. *Bulletin of Soil and Water Conservation*, 41 (3), 94-102 (in Chinese).